Impact of N-terminally substituted glucagon family receptor agonists on signal bias, trafficking and downstream responses

Ben Jones[1,#], Emma Rose McGlone[1], Zijian Fang[1], Phil Pickford[1], Ivan R Corrêa Jr[2], Sunil Kumar[3], Frederik Görlitz[3], Chris Dunsby[3], Paul MW French[3], Guy A Rutter[4], Tricia Tan[1], Alejandra Tomas[4,#], Stephen R Bloom[1].

1. Section of Endocrinology and Investigative Medicine, Imperial College London, London, United Kingdom.

2. New England Biolabs, Ipswich, USA

3. Department of Physics, Imperial College London, United Kingdom

4. Section of Cell Biology and Functional Genomics, Imperial College London, London, United Kingdom.

Corresponding authors: Ben Jones (ben.jones@imperial.ac.uk) and Alejandra Tomas (a.tomas-catala@imperial.ac.uk)

Keywords

Incretin, GLP-1, glucagon, GIP, trafficking, signal bias

Abbreviations

cAMP	Cyclic adenosine monophosphate
DERET	Diffusion-enhanced resonance energy transfer
DPP-4	Dipeptidyl dipeptidase-4
GCG	Glucagon
GCGR	Glucagon receptor
GIP	Glucose-dependent insulinotropic polypeptide
GIPR	Glucose-dependent insulinotropic polypeptide receptor
GLP-1	Glucagon-like peptide-1
GLP-1R	Glucagon-like peptide-1 receptor
NEP24.11	Neutral endopeptidase
T2D	Type 2 diabetes
TR-FRET	Time-resolved Förster resonance energy transfer

Abstract

Receptors for the peptide hormones glucagon-like peptide-1 (GLP-1), glucose-dependent insulinotropic polypeptide (GIP) and glucagon (GCG) are important regulators of insulin secretion and energy metabolism. Here we sought to investigate how signal bias between cyclic AMP and β-arrestin-2 recruitment can modulate the effects of prolonged agonist stimulation at each of these receptors. We generated analogues of GLP-1, GCG and GIP which in some cases showed selective reduction in β-arrestin-2 recruitment *versus* cAMP signalling compared to the parent peptide. Despite reduced acute signalling potency and/or efficacy, some biased GLP-1 and GIP analogues increased maximal sustained insulin secretion, although only at high agonist concentrations. Biased GCG analogues did not affect maximal insulin release from beta cells, or glucose output in hepatocytes.

1 Introduction

The receptors for the glucagon-like peptide-1 (GLP-1R), glucose-dependent insulinotropic polypeptide (GIPR) and glucagon (GCGR) are major pharmacological targets in metabolic diseases such as type 2 diabetes (T2D) and obesity [1]. Each of these receptors is present on pancreatic beta cells, and an important component of their overall metabolic actions when physiologically or pharmacologically activated is augmentation of glucose-stimulated insulin release [2,3]. In hepatocytes, GCGR facilitates glucose output, which may be undesirable in T2D; however, its "energy wasting" effect in peripheral tissues [2] could mitigate hyperglycaemia by weight loss and associated improvements in insulin sensitivity.

GLP-1R, GIPR and GCGR are closely related G protein-coupled receptors (GPCRs) in the class B (secretin) family. When activated, they engage the G protein $G\alpha_s$, which is coupled to insulin secretion via generation of cyclic adenosine monophosphate (cAMP) [4], and β-arrestins, which are multifunctional scaffold proteins widely reported to initiate non-G protein signalling cascades such as phosphorylation of mitogen-activated protein kinases (MAPKs) [5], and concurrently diminish G protein signalling by steric hindrance [6].

The balance between G protein and β-arrestin recruitment can be ligand-specific even at the same receptor – a pharmacological concept known as "biased signalling" [7]. A number of examples of signal bias at the GLP-1R have been described for naturally occurring [8,9] and pharmacological [10,11] orthosteric agonists. We recently described how biased GLP-1R agonists derived from exendin-4, characterised by reduced recruitment of β-arrestins, lead to increases in sustained insulin secretion through avoidance of GLP-1R desensitisation, reduction of GLP-1R endocytosis and resultant attenuation of GLP-1R downregulation over pharmacologically relevant time periods [12,13]. In view of the current drive to develop incretin analogues jointly targeting GLP-1R, GCGR and GIPR [1], we sought to establish whether signal bias could similarly be achieved at the latter two receptors, and to determine if this is associated with prolonged signalling responses, as seen at the GLP-1R.

In the present study, we report that a number of substitutions close to the N-terminus of the cognate ligand for each receptor result in reductions in both cAMP signalling and β-arrestin-2 recruitment, with bias in favour of cAMP in some cases. However, compared to our previous study with biased exendin-4 analogues at GLP-1R [12], the degree of bias achieved was more modest. Moreover, whilst bias-related differences were apparent in downstream responses such as insulin secretion, these were only apparent at high agonist concentrations.

2 Materials and methods

2.1 Peptides

All peptides were obtained from Insight Biotechnology and were at least 90% pure.

2.2 Cell lines

PathHunter β-arrestin-2 CHO-K1 cells (DiscoverX) stably expressing human GLP-1R, GIPR, or GCGR were maintained in the manufacturer's proprietary culture medium. HEK293T cells were maintained in DMEM, 10% FBS and 1% penicillin/streptomycin. INS-1 832/3 cells [14], a gift from Professor Christopher Newgard, were maintained in RPMI supplemented with 11 mM glucose, 10% FBS, 10 mM HEPES, 2 mM L-glutamine, 1 mM pyruvate, 50 μM β-mercaptoethanol and 1% penicillin/streptomycin. INS-1 832/3 cells lacking endogenous GLP-1R after deletion by CRISPR/Cas9 [15], a gift from Dr Jacqueline Naylor, AstraZeneca, were maintained similarly. A stable clone of Huh7 hepatoma cells expressing human GCGR was generated from a previously described multi-clonal cell population [16] by flow cytometric sorting of cells labelled with FITC-conjugated glucagon, and subsequently maintained in DMEM, 10% FBS, 1% penicillin/streptomycin and 1 mg/ml G418.

2.3 Transfections

Transient transfections of plasmid DNA containing the SNAP-tagged human GLP-1R, GIPR or GCGR (Cisbio) were performed using Lipofectamine 2000 according to the manufacturer's recommendations; unless indicated, cells were assayed 24 hours after DNA transfection.

2.4 Isolation of primary hepatocytes

Hepatocytes from adult male C57Bl/6J mice were isolated using collagenase perfusion [17]. After filtering and washing, cells were plated in 12-well collagen-coated plates at 3x 10^5 cells/ml, 1 ml per well in attachment medium (M199 with 1% penicillin/streptomycin, 1% BSA, 10% FBS, 100 nM triiodothyronine, 100 nM dexamethasone and 100 nM insulin). After 5 hours, attachment medium was

replaced with serum starvation medium (M199 with 1% penicillin/streptomycin, 100 nM dexamethasone and 10 nM insulin).

2.5 Cyclic AMP assays

All experiments were performed at 37°C. PathHunter CHO-K1 cells: Cells were resuspended in serum-free Ham's F12 medium and treated with indicated agonist, without phosphodiesterase inhibitors, for 30 minutes, followed by application of detection reagents for determination of cAMP by HTRF (cAMP Dynamic 2, Cisbio). β-arrestin-2 recruitment responses (section 2.6) were measured in parallel. Huh7-GCGR cells were treated with indicated concentration of agonist without phosphodiesterase inhibitors before lysis. Curve fitting was performed using Prism 8.0 (Graphpad Software).

2.6 β-arrestin recruitment assay

β-arrestin-2 recruitment was determined by enzyme fragment complementation using the PathHunter system (DiscoverX). CHO-K1 cells expressing GLP-1R, GIPR or GCGR were treated with indicated concentrations of agonist for 30 minutes at 37°C before addition of detection reagents.

2.7 Measurement of receptor internalisation by DERET

Diffusion-enhanced resonance energy transfer (DERET) [18] was used to monitor agonist-induced receptor internalisation in transiently transfected HEK293T cells (24 hours after DNA transfection of N-terminally SNAP-tagged receptors), or in monoclonal stably transfected CHO-K1 cells. Labelling was performed using the time-resolved Förster resonance energy transfer (TR-FRET) SNAP-probe Lumi4-Tb (Cisbio) at 40 nM for 60 minutes at room temperature, either in suspension (for HEK293T) or with adherent cells (for CHO-K1). After washing three times, fluorescein (24 μM in HBSS) was added to cells in opaque bottom white plates, and baseline signal was read for 10 minutes using a Flexstation 3 plate reader (λ_{ex} 340 nm, λ_{em} 520 and 620 nm, delay 400 μs, integration 1500 μs) at 37°C. Agonists, prepared in 24 μM fluorescein, were added, and signal was sequentially monitored. Receptor endocytosis leads to reduced contact of Lumi4-Tb with extracellular fluorescein, and a

reduction in signal at 520 nm with an increase at 620 nm. After first subtracting values from wells containing fluorescein only, internalisation was expressed ratiometrically as signal obtained at 620 nm divided by that obtained at 520 nm.

2.8 Measurement of receptor internalisation using a cleavable SNAP-labelling probe

The assay was adapted from a previous description [13]. HEK293T cells were seeded in black, clear bottom, plates coated with 0.1% poly-D-lysine and assayed 24 hours after transfection with plasmid DNA. Cells were labelled with the cleavable SNAP-tag probe BG-S-S-649 (featuring the DY-649 fluorophore, a gift from New England Biolabs) in complete medium for 30 minutes at room temperature. After washing, fresh medium ± agonist was added, with agonists applied in reverse time order in the case of time-course experiments. At the end of the incubation, medium was removed and wells were treated with for 10 minutes at 4°C with Mesna (100 mM, in alkaline TNE buffer, pH 8.6), or with alkaline TNE buffer alone, to remove BG-S-S-649 bound to residual surface receptor without affecting the internalised receptor population. After washing, cells were imaged using an automated Nikon Ti2 widefield microscope with LED light source (CoolLED) and a 0.75 numerical aperture 20X air objective, assisted by custom-written high content analysis software [19] implemented in Micro-Manager [20]. A minimum of 4 epifluorescence and matching transmitted phase contrast images per well were acquired. Average internalised receptor across the imaged cell population was quantified using Fiji as follows: 1) phase contrast images were processed using PHANTAST [21] to segment cell-containing regions from background; 2) illumination correction of fluorescence images was performed using BaSiC [22]; 3) fluorescence intensity was quantified for cell-containing regions. Agonist-mediated internalisation was determined by comparing the mean signal for each condition normalised to signal from wells not treated with Mesna, after first subtracting non-specific fluorescence determined from wells treated with Mesna but no agonist.

2.9 Gene expression analysis

RNA was harvested from INS-1 832/3 and Huh7 cells using the Cells-to-CT kit (Themo Fisher). Taqman probes were used to detect expression of *Glp1r* (Rn00562406_m1), *Gipr* (Rn00562325_m1),

Gcgr (Rn00597162_g1), *G6pc* (Rn00689876_m1) and endogenous control gene 18S (Hs99999901_s1) by quantitative PCR.

2.10 Insulin secretion

Insulin secretion from INS-1 832/3 cells [14] was assayed after a prior overnight period of exposure to low glucose (3 mM) complete medium. Cells were added in suspension to plates containing indicated agonists, prepared in RPMI containing 2% FBS and 11 mM glucose, for 16 hours. Supernatant insulin concentration was determined by HTRF (High Range Insulin kit, Cisbio). Results were normalised to those obtained with 11 mM glucose but no additional agonist. Three-parameter fitting was performed using Prism 8.0.

2.11 Glucose production

Overnight serum-starved hepatocytes were washed and glucose production medium (phenol-red free DMEM containing 1mM pyruvate and 20mM lactate) was applied. After 24 hours exposure to agonist, media was assayed for glucose content using a glucose oxidase method (GLUC-PAP, Randox). Glucose content was normalised to protein content of each well (BCA assay).

2.12 Data analysis and statistics

All analyses were performed using Prism 8.0. For bias calculations, to reduce contribution of inter-assay variability, cAMP and β-arrestin-2 assays were performed concurrently, with the same incubation time of 30 minutes to avoid artefactual bias resulting from different activation kinetics of each pathway [23]; bias was determined by calculating transduction coefficients [24,25]; here, due to the matched design of our experiments, we calculated $\Delta\Delta\log(\tau/K_A)$ on a per-assay basis by normalising the $\log(\tau/K_A)$ of each ligand to the relevant endogenous ligand (GLP-1, GIP or GCG, to generate a $\Delta\log[\tau/K_A]$ value) and then to the reference pathway (cAMP). All experiments had a matched design, allowing paired, two-tailed t-tests, or randomised block one-way ANOVA to be performed. Specific statistical tests are indicated in the figure legends. Statistical significance was inferred when $p<0.05$. To determine statistical significance for signal bias, 95% confidence intervals

were calculated; bias *versus* the reference endogenous ligand was considered statistically significant when this confidence interval did not cross zero, as previously recommended [24].

3 Results

3.1 Effects of N-terminal region mutations to GLP-1, GIP and glucagon on signalling

Biased signalling, in which agonists preferentially stabilise certain receptor conformations to engage specific intracellular signalling pathways, may provide a means to selectively increase therapeutic effects [26]. As the ligand N-terminal region plays a key role in activation of class B GPCRs [27] and is linked to GLP-1R biased signalling [12], we introduced single amino acid substitutions at or close to the N-termini of each endogenous ligand (Table 1 for full amino acid sequences) and tested for intracellular cAMP production (Figure 1A) and β-arrestin-2 recruitment (Figure 1B). For each receptor target, all N-terminally modified analogues retained full efficacy for cAMP, but with reduced potency (full parameter estimates are given in Table 2). Potency for β-arrestin-2 recruitment was also reduced, and in the majority of cases, a reduction in efficacy was also observed. Transduction ratios [25] were calculated to quantify the relative signalling impact of each N-terminal region substitution in each ligand for each pathway (Figure 1C, D). Chiral substitution of the first amino acid to dHis1 (GLP-1, GCG) or dTyr1 (GIP), as well as Gly2 and dGln3, were less well tolerated by GIP and GCG than by GLP-1; for example, GIP-dGln3 showed a 100-fold reduction in cAMP potency compared to wild-type GIP, *versus* a 10-fold reduction seen for GLP-1-dGln3 compared to GLP-1. Moreover, comparison of the relative impact of each substitution on cAMP *versus* β-arrestin-2 responses showed that all compounds tested exhibited at least a trend for bias in favour of G protein-dependent cAMP signalling, albeit not statistically significant (as indicated by 95% confidence intervals crossing zero) in some cases (Figure 1E). The large error bars for the bias estimate for GIP-dGln3 reflect the limitations of this method for bias calculation for extremely weak partial agonists [28].

Overall, these results highlight how the N-termini of each ligand play important roles in receptor activation. However, it should be noted that the magnitude of signal bias with the GLP-1 analogues tested here is smaller than for exendin-4-derived biased GLP-1R agonists, a finding that is consistent with our recent exploration of GLP-1/exendin-4 chimeric peptides [13].

3.2 Receptor endocytosis induced by biased incretin receptor agonists

β-arrestin recruitment is classically linked to GPCR endocytosis [29], although conflicting evidence exists for a direct role in controlling trafficking of incretin receptors [30-34]. Nevertheless, a clear correlation between β-arrestin recruitment and GLP-1R internalisation with biased GLP-1R agonists has been demonstrated [12]. We therefore used diffusion-enhanced resonance energy transfer (DERET) [35] to monitor agonist-induced loss of surface labelled SNAP-tagged receptors transiently expressed in HEK293T cells. Robust internalisation was noted for GLP-1R stimulated with GLP-1. In contrast, GIPR internalisation with GIP was less extensive, and no change in DERET signal could be detected with GCGR stimulated by GCG (Figure 2A). Endocytic profiles were confirmed using an alternative approach based on reversible SNAP-tag labelling, in which the fluorescent probe BG-S-S-649 is cleaved from residual surface receptors after agonist-induced internalisation using the cell-impermeant reducing agent Mesna [13,36]. A time course study showed rapid and extensive loss of surface SNAP-GLP-1R when cells were treated with GLP-1, whereas SNAP-GIPR and SNAP-GCGR internalisation with their cognate agonists were, respectively, more limited and virtually absent (Figure 2B). Representative images showing the effect of Mesna cleavage are shown in Figure 2C.

We compared GLP-1R and GIPR internalisation induced by the N-terminally substituted agonists described in Figure 1, finding that in all cases receptor internalisation was reduced when measured by DERET using stably transfected CHO-K1 cells expressing SNAP-GLP-1R or SNAP-GIPR (Figure 2D, E). The reversible SNAP-tag labelling assay showed a similar pattern (Figure 2F). The GCG analogues were not studied with this assay as GCG itself was without effect.

3.3 Responses in the beta cell context

As pancreatic beta cells are a target for GLP-1, GIP and GCG [37], we investigated whether the signalling and trafficking characteristics of N-terminally modified agonists described above could enhance insulin secretion, as previously demonstrated for biased exendin-4-derived GLP-1RAs [12]. We used incretin-responsive rat insulinoma-derived INS-1 832/3 cells [14], in which we first confirmed expression of GLP-1R, GIPR and GCGR by qPCR (Figure 3A). Using N-terminally substituted GLP-

1 and GIP analogues, we found subtly increased maximal sustained insulin secretion with a number of analogues compared to their respective parent ligand, but this was only apparent at concentrations above 1 μM (Figure 3B, C, Table 3). The majority of analogues displayed reduced potency for insulin secretion, as they had for acute cAMP production in the signalling assays presented in Figure 1, except for GLP-1-gly2, which is likely to reflect protection against DPP-4-mediated degradation with this ligand. For GIP analogues, maximal insulin secretion was correlated with maximal β-arrestin-2 recruitment; for GLP-1 analogues the relationship was less clear (Figure 3D). As GCG can cross-react with GLP-1R in beta cells [38], we tested each N-terminally modified GCG analogue in both wild-type INS-1 832/3 cells and a sub-clone in which GLP-1R had been knocked out by CRISPR/Cas9 [15]. This showed that the overall response was dominated by GLP-1R-dependent high dose effects absent in GLP-1R knockout cells, with no clear GCGR-dependent advantageous effect for any analogue (Figure 3E).

Overall, these results indicate that analogues of GLP-1 and GIP with reduced β-arrestin-2 recruitment can augment glucose-stimulated insulin secretion, but with the peptides evaluated in this study, this effect was only apparent at high agonist concentrations.

3.4 Responses to biased GCG analogues in the hepatocyte context

GCG stimulates glycogenolysis and gluconeogenesis in hepatocytes. Recently, ablation of β-arrestin-2 in hepatocytes was found to increase hepatic glucose output in response to GCG [33]. We used Huh7 cells stably expressing GCGR ("Huh7-GCGR") [16] to assess responses to prolonged stimulation with biased GCG analogues, to determine if differences in β-arrestin recruitment could affect sustained GCGR signalling in a hepatocyte context. Comparisons of maximum cAMP accumulation after 16-hour stimulation with each ligand revealed that greater efficacy for cAMP production was achieved by ligands with reduced β-arrestin-2 recruitment (Figure 4A, Table 3); and in the case of the -Phe1 and -dGln3 compounds, cAMP potency was also greater than for GCG, despite being at least 10-fold less potent acutely (see Figure 1). However, this did not translate to differential changes in GCGR-induced upregulation of the gluconeogenic enzyme glucose-6-

phosphatase (G6P; Figure 4B); neither were any significant differences seen for production of glucose in primary mouse hepatocytes (Figure 4C).

4 Discussion

This study builds on our earlier work using biased GLP-1R agonists derived from exendin-4 and GLP-1 bearing amino acid substitutions close to the N-terminus [12,13]. In the former study [12], we found that a number of changes, including dHis1, dTyr1, Phe1 and dGln3 (as included in the present investigation) led to marked reductions in recruitment of β-arrestin-1 and -2, substantially reduced GLP-1R endocytosis, increased insulin secretion, and improved anti-hyperglycaemic effect in mice. In the latter study [13] we observed that the Phe1 substitutions led to less marked improvements in insulin secretion in a GLP-1 *versus* exendin-4 context. We therefore sought to expand this concept to the related class B GPCR targets in the present study, which are structurally and functionally related to the GLP-1R and of interest as therapeutic targets in metabolic disease [39]. Overall, our new data indicate that amino acid substitutions at or close to the N-termini of GLP-1, GIP and GCG can indeed diminish β-arrestin-2 recruitment efficacy, with a somewhat lesser effect on cAMP signalling, but that the degree of pathway selectivity is reduced compared to what we have previously observed with exendin-4 analogues at the GLP-1R [12]. Moreover, the impact on prolonged insulin secretion in pancreatic beta cells was more limited.

GLP-1 is more dependent on its N-terminus for binding to the GLP-1R than is exendin-4 [40]. Sequential truncation of the first nine amino acids of exendin-4 results in only a modest reduction in binding affinity, but virtually abolishes binding of GLP-1 [41,42]. Thus, the reduction in signalling potency resulting from an N-terminal amino acid substitution within the GLP-1 backbone may be secondary to reduced affinity, whereas within exendin-4, the same change might have little impact on occupancy, thereby allowing the modified ligand to achieve biased signalling at higher potency. Verifying this concept, acute cAMP signalling potencies for exendin-dHis1 and exendin-Phe1 in our earlier study were, respectively, no different to and 2.5-fold lower than for exendin-4 [12]. In contrast, in the present work, the same substitutions to the GLP-1 N-terminus reduced cAMP potency by, respectively, a factor of 6 and 10. This might limit the potential for these modified GLP-1 analogues to improve downstream signalling outputs during prolonged stimulation, except at maximal doses when receptor occupancy is high. As for GLP-1, the N-termini of both GCG and GIP are also known

to play a major role in affinity for their cognate receptors, with truncation of the terminal amino acid residue resulting in a >10-fold loss of affinity in both cases [43,44].

A number of the analogues tested in this report have previously been described, due in part to the interest in reducing ligand sensitivity to degradation by the N-terminal targeting exopeptidase DPP-4 [45]. Published potency or affinity measures for GLP-1-dHis1 [46] and -Gly2 [47] were broadly in agreement with our results, although GLP-1-Phe1 was found to be well tolerated for cAMP signalling potency in RIN-T3 cells [48], contrasting with the deleterious effect we observed. Differences in cell type, receptor species, incubation times and other factors may influence responses to agonists, complicating direct comparisons with reported values in the literature [23]. The affinity of GIP-dTyr1 was reduced 10-fold compared to unmodified GIP [49], similar to our results, whereas the -Gly2 substitution was well tolerated [50]. GIP-Phe1 has been used as a GIPR I^{125}-radioligand [51]. These datasets are complemented here by our measures of bias between cAMP and β-arrestin recruitment, and endocytosis, which have not previously been reported for these ligands, or indeed for any putative biased GCGR or GIPR agonists to our knowledge.

A further factor which might contribute to the relative lack of effect on downstream responses to biased GLP-1, GIP and GCG analogues during prolonged incubations is enzymatic peptide degradation, for example by neutral endopeptidase 24.11 (NEP 24.11), found on pancreatic beta cell membranes and capable of hydrolysing GLP-1, GCG, and to a lesser extent, GIP [52], or endothelin converting enzyme-1 [53] situated predominantly in endosomal compartments. DPP-4, also expressed by beta cells [54], is also likely to contribute, although the modified N-termini of the ligands tested may confer some resistance to its action. Sequence optimisation to increase proteolytic stability during our extended *in vitro* studies may be required to maintain adequate ligand concentration to fully manifest consequences of signal bias. In the *in vivo* setting, fatty acid conjugation e.g. liraglutide [55] protects against NEP 24.11 and DPP-4 degradation, presumably as the resultant albumin-bound form of the ligand is inaccessible to the enzymes. One possible future approach would be to test acylated forms

of the ligands described herein to determine if sustained exposure to the N-terminally substituted forms led to enhanced metabolic effects.

In summary, we demonstrate in this study that GLP-1, GIP and GCG analogues with a variety of N-terminal substitutions typically show reduced β-arrestin-2 recruitment. In the case of GLP-1 and GIP, this is associated with reduced receptor endocytosis, and this effect can be exploited to increase maximal insulin release *in vitro*. Generation of long-lasting biased incretin mimetics will be required to determine whether this applies *in vivo*.

Table 1. Amino acid sequences of ligands in this study.

Ligand	Sequence
GLP-1-derived ligands	
GLP-1(7-36)NH_2	HAEGTFTSDVSSYLEGQAAKEFIAWLVKGR-NH_2
GLP-1-dHis1	(dH)AEGTFTSDVSSYLEGQAAKEFIAWLVKGR-NH_2
GLP-1-Phe1	FAEGTFTSDVSSYLEGQAAKEFIAWLVKGR-NH_2
GLP-1-Gly2	HGEGTFTSDVSSYLEGQAAKEFIAWLVKGR-NH_2
GLP-1-dGln3	HA(dQ)GTFTSDVSSYLEGQAAKEFIAWLVKGR-NH_2
GIP-derived ligands	
GIP(1-42)	YAEGTFISDYSIAMDKIHQQDFVNWLLAQKGKKNDWKHNITQ
GIP-dTyr1	(dY)AEGTFISDYSIAMDKIHQQDFVNWLLAQKGKKNDWKHNITQ
GIP-Phe1	FAEGTFISDYSIAMDKIHQQDFVNWLLAQKGKKNDWKHNITQ
GIP-Gly2	YGEGTFISDYSIAMDKIHQQDFVNWLLAQKGKKNDWKHNITQ
GIP-dGln3	YA(dQ)GTFISDYSIAMDKIHQQDFVNWLLAQKGKKNDWKHNITQ
GCG-derived ligands	
GCG(1-29)	HSQGTFTSDYSKYLDSRRAQDFVQWLMNT
GCG-dHis1	dHSQGTFTSDYSKYLDSRRAQDFVQWLMNT
GCG-Phe1	FSQGTFTSDYSKYLDSRRAQDFVQWLMNT
GCG-Gly2	HGQGTFTSDYSKYLDSRRAQDFVQWLMNT
GCG-dGln3	HSdQGTFTSDYSKYLDSRRAQDFVQWLMNT

Table 2. Pharmacological characterisation of biased GLP-1R, GIPR and GCGR agonists.

Parameter estimates ± SEM from responses depicted in Figure 1. * p<0.05, by one-way randomised block ANOVA with Dunnett's test *vs.* GLP-1, GIP and glucagon, as appropriate. Note that for E_{max}, statistical comparison was performed prior to normalisation.

	cAMP					**βarr2**				
GLP-1R	**GLP-1**	**dHis1**	**Phe1**	**Gly2**	**dGln3**	**GLP-1**	**dHis1**	**Phe1**	**Gly2**	**dGln3**
E_{max} (% GLP-1)	100	101 ± 4	100 ± 4	95 ± 4	106 ± 5	100	66 ± 5 *	48 ± 6 *	93 ± 3	60 ± 4 *
Log EC_{50}	-9.5 ± 0.2	-8.7 ± 0.2 *	-8.5 ± 0.2 *	-9.2 ± 0.2 *	-8.6 ± 0.2 *	-6.5 ± 0.2	-5.9 ± 0.1 *	-5.8 ± 0.0 *	-5.9 ± 0.1 *	-5.8 ± 0.0 *
Hill Slope	1.7 ± 0.4	1.4 ± 0.3	1.4 ± 0.1	1.4 ± 0.1	1.7 ± 0.5	0.8 ± 0.1	2.0 ± 0.2 *	2.1 ± 0.2 *	1.0 ± 0.1	2.0 ± 0.3 *
Log (τ/KA)	9.5 ± 0.2	8.7 ± 0.1 *	8.5 ± 0.2 *	9.2 ± 0.2 *	8.6 ± 0.2 *	6.5 ± 0.1 *	5.6 ± 0.1 *	5.3 ± 0.1 *	5.9 ± 0.1 *	5.4 ± 0.1 *
GIPR	**GIP**	**dTyr1**	**Phe1**	**Gly2**	**dGln3**	**GIP**	**dTyr1**	**Phe1**	**Gly2**	**dGln3**
E_{max} (% GIP)	100	96 ± 6	99 ± 3	100 ± 4	110 ± 4	100	52 ± 6 *	65 ± 3 *	66 ± 7 *	23 ± 1 *
Log EC_{50}	-10.0 ± 0.2	-8.5 ± 0.2 *	-8.7 ± 0.2 *	-9.1 ± 0.2 *	-7.6 ± 0.3 *	-7.1 ± 0.1	-6.3 ± 0.2 *	-6.0 ± 0.1 *	-6.5 ± 0.3	-6.5 ± 0.3
Hill Slope	1.4 ± 0.1	1.3 ± 0.2	1.2 ± 0.1	1.6 ± 0.4	1.0 ± 0.1	0.6 ± 0.1	1.1 ± 0.1	1.2 ± 0.2	1.0 ± 0.2	85.7 ± 53.1
Log (τ/KA)	9.9 ± 0.2	8.5 ± 0.3 *	8.6 ± 0.2 *	9.1 ± 0.2 *	7.7 ± 0.3 *	7.2 ± 0.1	5.2 ± 0.2 *	5.5 ± 0.1 *	5.9 ± 0.1 *	4.0 ± 0.6 *
GCGR	**GCG**	**dHis1**	**Phe1**	**Gly2**	**dGln3**	**GCG**	**dHis1**	**Phe1**	**Gly2**	**dGln3**
E_{max} (% GCG)	100	108 ± 5	93 ± 2	99 ± 5	101 ± 5	100	85 ± 4 *	84 ± 4 *	43 ± 4 *	85 ± 4 *
Log EC_{50}	-9.8 ± 0.2	-8.2 ± 0.2 *	8.9 ± 0.2 *	-8.1 ± 0.1 *	-8.3 ± 0.1 *	-7.4 ± 0.3	-5.9 ± 0.1 *	-6.4 ± 0.1 *	-5.8 ± 0.1 *	-5.8 ± 0.1 *
Hill Slope	1.4 ± 0.1	1.4 ± 0.2	1.6 ± 0.1	1.7 ± 0.2	1.5 ± 0.1	0.6 ± 0.1	1.8 ± 0.2 *	1.7 ± 0.5 *	2.9 ± 0.4 *	1.8 ± 0.2 *
Log (τ/KA)	9.8 ± 0.2	8.3 ± 0.1 *	8.8 ± 0.2 *	8.1 ± 0.1 *	8.3 ± 0.1 *	7.6 ± 0.2	5.8 ± 0.1 *	6.5 ± 0.1 *	5.3 ± 0.1 *	5.8 ± 0.1 *

Table 3. Responses to N-terminally substituted ligands in INS-1 832/3 and Huh7-GCGR cells. Parameter estimates ± SEM from insulin secretory responses depicted in Figure 3F-H and 16-hour cAMP accumulation in Figure 4A. Note that the Hill slopes for GCG analogues in Huh7-GCGR cells are derived from the curves plotted from the pooled data, so no statistical comparisons are shown. * $p<0.05$, by one-way randomised block ANOVA with Dunnett's test *vs.* GLP-1, GIP and glucagon, as appropriate. "n.c." indicates not calculated.

	GLP-1 analogues - wild-type INS-1 832/3 cells				
	GLP-1	**dHis1**	**Phe1**	**Gly2**	**dGln3**
E_{max}	4.0 ± 0.7	3.8 ± 0.8	4.9 ± 0.8 *	3.8 ± 0.6	5.0 ± 1.0 *
Log EC_{50}	-8.5 ± 0.1	-8.6 ± 0.0	-7.4 ± 0.1 *	-9.2 ± 0.1 *	-7.5 ± 0.1 *
	GIP analogues - wild-type INS-1 832/3 cells				
	GIP	**dTyr1**	**Phe1**	**Gly2**	**dGln3**
E_{max}	4.2 ± 0.2	4.9 ± 0.3 *	5.1 ± 0.4 *	5.0 ± 0.3 *	5.4 ± 0.3 *
Log EC_{50}	-8.3 ± 0.1	-7.4 ± 0.1 *	-6.9 ± 0.2 *	-7.8 ± 0.1 *	-6.4 ± 0.1 *
	GCG analogues – wild-type INS-1 832/3 cells				
	GCG	**dHis1**	**Phe1**	**Gly2**	**dGln3**
E_{max}	n.c	n.c	n.c	n.c	n.c
Log EC_{50}	n.c	n.c	n.c	n.c	n.c
	GCG analogues – GLP-1R KO INS-1 832/3 cells				
	GCG	**dHis1**	**Phe1**	**Gly2**	**dGln3**
E_{max}	1.3 ± 0.1	1.4 ± 0.1	1.5 ± 0.2	1.6 ± 0.2	1.5 ± 0.2
Log EC_{50}	-7.2 ± 0.5	-7.3 ± 0.3	-7.0 ± 0.8	-6.9 ± 0.4	-6.5 ± 0.5
	GCG analogues – Huh7-GCGR cells				
	GCG	**dHis1**	**Phe1**	**Gly2**	**dGln3**
E_{max}	46 ± 1	64 ± 2 *	64 ± 4 *	64 ± 4 *	67 ± 4 *
Log EC_{50}	-8.8 ± 0.0	-8.6 ± 0.0 *	-9.0 ± 0.1 *	-8.4 ± 0.0 *	-9.1 ± 0.0 *
Hill slope	1.9	3.4	2.8	3.0	3.0

Funding sources

This work was funded by an MRC project grant to B.J., A.T., S.R.B. and G.A.R. The Section of Endocrinology and Investigative Medicine is funded by grants from the MRC, BBSRC, NIHR, an Integrative Mammalian Biology (IMB) Capacity Building Award, an FP7-HEALTH-2009-241592 EuroCHIP grant and is supported by the NIHR Biomedical Research Centre Funding Scheme. The views expressed are those of the author(s) and not necessarily those of the funder. B.J. was also supported for this work by the Academy of Medical Sciences, Society for Endocrinology and an EPSRC capital award. G.A.R. was supported by Wellcome Trust Investigator (212625/Z/18/Z) Awards, MRC Programme (MR/R022259/1) and Experimental Challenge Grant (DIVA, MR/L02036X/1), and Diabetes UK (BDA/11/0004210, BDA/15/0005275, BDA 16/0005485) grants. This work has received support from the EU/EFPIA/Innovative Medicines Initiative 2 Joint Undertaking (RHAPSODY grant No 115881) to G.A.R.

Author contributions

BJ, SRB and AT conceived and designed the study. BJ, ERM, ZF and PP performed and analysed experiments. IRC provided novel reagents. SK, FG, CD and PMWF developed HCA instrumentation and analysis tools. Funding for the study was acquired by BJ, AT, SRB, GAR and TT. BJ wrote the draft manuscript. All authors made manuscript revisions and approved the final version.

Conflict of interest statement

GAR is a consultant for Sun Pharmaceuticals and has received grant funding from Sun Pharmaceuticals and Les Laboratoires Servier. BJ and AT have received grant funding from Sun Pharmaceuticals.

References

1 Finan B, Yang B, Ottaway N, Smiley DL, Ma T, Clemmensen C, Chabenne J, Zhang L, Habegger KM, Fischer K, Campbell JE, Sandoval D, Seeley RJ, Bleicher K, Uhles S, Riboulet W, Funk J, Hertel C, Belli S, Sebokova E, Conde-Knape K, Konkar A, Drucker DJ, Gelfanov V, Pfluger PT, Müller TD, Perez-Tilve D, Dimarchi RD & Tschöp MH (2014) A rationally designed monomeric peptide triagonist corrects obesity and diabetes in rodents. *Nat Med*.

2 Tan TM, Field BCT, McCullough KA, Troke RC, Chambers ES, Salem V, Gonzalez Maffe J, Baynes KCR, De Silva A, Viardot A, Alsafi A, Frost GS, Ghatei MA & Bloom SR (2013) Coadministration of glucagon-like peptide-1 during glucagon infusion in humans results in increased energy expenditure and amelioration of hyperglycemia. *Diabetes* **62**, 1131–1138.

3 Nauck MA & Meier JJ (2016) The incretin effect in healthy individuals and those with type 2 diabetes: physiology, pathophysiology, and response to therapeutic interventions. *Lancet Diabetes Endocrinol* **4**, 525–536.

4 Dyachok O, Isakov Y, Sågetorp J & Tengholm A (2006) Oscillations of cyclic AMP in hormone-stimulated insulin-secreting beta-cells. *Nature* **439**, 349–352.

5 Pierce KL, Maudsley S, Daaka Y, Luttrell LM & Lefkowitz RJ (2000) Role of endocytosis in the activation of the extracellular signal-regulated kinase cascade by sequestering and nonsequestering G protein-coupled receptors. *Proc Natl Acad Sci USA* **97**, 1489–1494.

6 Benovic JL, Kühn H, Weyand I, Codina J, Caron MG & Lefkowitz RJ (1987) Functional desensitization of the isolated beta-adrenergic receptor by the beta-adrenergic receptor kinase: potential role of an analog of the retinal protein arrestin (48-kDa protein). *Proc Natl Acad Sci USA* **84**, 8879–8882.

7 Kenakin T (2018) Is the Quest for Signaling Bias Worth the Effort? *Mol. Pharmacol.* **93**, 266–269.

8 Jorgensen R, Kubale V, Vrecl M, Schwartz TW & Elling CE (2007) Oxyntomodulin differentially affects glucagon-like peptide-1 receptor beta-arrestin recruitment and signaling through Galpha(s). *J Pharmacol Exp Ther* **322**, 148–154.

9 Fletcher MM, Halls ML, Zhao P, Clydesdale L, Christopoulos A, Sexton PM & Wootten D (2018) Glucagon-like peptide-1 receptor internalisation controls spatiotemporal signalling mediated by biased agonists. *Biochem. Pharmacol.* **156**, 406–419.

10 Zhang H, Sturchler E, Zhu J, Nieto A, Cistrone PA, Xie J, He L, Yea K, Jones T, Turn R, Di Stefano PS, Griffin PR, Dawson PE, McDonald PH & Lerner RA (2015) Autocrine selection of a GLP-1R G-protein biased agonist with potent antidiabetic effects. *Nat Commun* **6**, 8918–13.

11 Hager MV, Johnson LM, Wootten D, Sexton PM & Gellman SH (2016) β-Arrestin-Biased Agonists of the GLP-1 Receptor from β-Amino Acid Residue Incorporation into GLP-1 Analogues. *J. Am. Chem. Soc.* **138**, 14970–14979.

12 Jones B, Buenaventura T, Kanda N, Chabosseau P, Owen BM, Scott R, Goldin R, Angkathunyakul N, Corrêa IR, Bosco D, Johnson PR, Piemonti L, Marchetti P, Shapiro AMJ, Cochran BJ, Hanyaloglu AC, Inoue A, Tan T, Rutter GA, Tomas A & Bloom SR (2018) Targeting GLP-1 receptor trafficking to improve agonist efficacy. *Nat Commun* **9**, 1602.

13 Fang Z, Chen S, Pickford P, Broichhagen J, Hodson DJ, Corrêa IR Jr, Kumar S, Görlitz F, Dunsby C, French PMW, Rutter GA, Tan T, Bloom SR, Tomas A & Jones B (2020) The influence of peptide context on signalling and trafficking of glucagon-like peptide-1 receptor biased agonists. *ACS Pharmacol. Transl. Sci.*, acsptsci.0c00022.

14 Hohmeier HE, Mulder H, Chen G, Henkel-Rieger R, Prentki M & Newgard CB (2000) Isolation of INS-1-derived cell lines with robust ATP-sensitive K+ channel-dependent and -independent glucose-stimulated insulin secretion. *Diabetes* **49**, 424–430.

15 Naylor J, Suckow AT, Seth A, Baker DJ, Sermadiras I, Ravn P, Howes R, Li J, Snaith MR, Coghlan MP & Hornigold DC (2016) Use of CRISPR/Cas9-engineered INS-1 pancreatic β cells to define the pharmacology of dual GIPR/GLP-1R agonists. *Biochem J* **473**, 2881–2891.

16 Cegla J, Jones BJ, Gardiner JV, Hodson DJ, Marjot T, McGlone ER, Tan TM & Bloom SR (2017) RAMP2 Influences Glucagon Receptor Pharmacology via Trafficking and Signaling. *Endocrinology* **158**, 2680–2693.

17 Johanns M, Lai Y-C, Hsu M-F, Jacobs R, Vertommen D, Van Sande J, Dumont JE, Woods A, Carling D, Hue L, Viollet B, Foretz M & Rider MH (2016) AMPK antagonizes hepatic glucagon-

stimulated cyclic AMP signalling via phosphorylation-induced activation of cyclic nucleotide phosphodiesterase 4B. *Nat Commun* **7**, 10856.
18 Roed SN, Wismann P, Underwood CR, Kulahin N, Iversen H, Cappelen KA, Schäffer L, Lehtonen J, Hecksher-Soerensen J, Secher A, Mathiesen JM, Bräuner-Osborne H, Whistler JL, Knudsen SM & Waldhoer M (2014) Real-time trafficking and signaling of the glucagon-like peptide-1 receptor. *Mol Cell Endocrinol* **382**, 938–949.
19 High Content Analysis High Content Analysis.
20 Edelstein A, Amodaj N, Hoover K, Vale R & Stuurman N (2010) Computer control of microscopes using µManager. *Curr Protoc Mol Biol* **Chapter 14**, Unit14.20.
21 Jaccard N, Griffin LD, Keser A, Macown RJ, Super A, Veraitch FS & Szita N (2014) Automated method for the rapid and precise estimation of adherent cell culture characteristics from phase contrast microscopy images. *Biotechnol. Bioeng.* **111**, 504–517.
22 Peng T, Thorn K, Schroeder T, Wang L, Theis FJ, Marr C & Navab N (2017) A BaSiC tool for background and shading correction of optical microscopy images. *Nat Commun* **8**, 14836–7.
23 Klein Herenbrink C, Sykes DA, Donthamsetti P, Canals M, Coudrat T, Shonberg J, Scammells PJ, Capuano B, Sexton PM, Charlton SJ, Javitch JA, Christopoulos A & Lane JR (2016) The role of kinetic context in apparent biased agonism at GPCRs. *Nat Commun* **7**, 10842.
24 Kenakin T, Watson C, Muniz-Medina V, Christopoulos A & Novick S (2012) A simple method for quantifying functional selectivity and agonist bias. *ACS Chem Neurosci* **3**, 193–203.
25 van der Westhuizen ET, Breton B, Christopoulos A & Bouvier M (2014) Quantification of ligand bias for clinically relevant β2-adrenergic receptor ligands: implications for drug taxonomy. *Mol. Pharmacol.* **85**, 492–509.
26 Schmid CL, Kennedy NM, Ross NC, Lovell KM, Yue Z, Morgenweck J, Cameron MD, Bannister TD & Bohn LM (2017) Bias Factor and Therapeutic Window Correlate to Predict Safer Opioid Analgesics. *Cell* **171**, 1165–1175.e13.
27 Wootten D, Reynolds CA, Smith KJ, Mobarec JC, Koole C, Savage EE, Pabreja K, Simms J, Sridhar R, Furness SGB, Liu M, Thompson PE, Miller LJ, Christopoulos A & Sexton PM (2016) The Extracellular Surface of the GLP-1 Receptor Is a Molecular Trigger for Biased Agonism. *Cell* **165**, 1632–1643.
28 Stahl EL, Zhou L, Ehlert FJ & Bohn LM (2015) A novel method for analyzing extremely biased agonism at G protein-coupled receptors. *Mol. Pharmacol.* **87**, 866–877.
29 Goodman OB, Krupnick JG, Santini F, Gurevich VV, Penn RB, Gagnon AW, Keen JH & Benovic JL (1996) Beta-arrestin acts as a clathrin adaptor in endocytosis of the beta2-adrenergic receptor. *Nature* **383**, 447–450.
30 Jorgensen R, Martini L, Schwartz TW & Elling CE (2005) Characterization of glucagon-like peptide-1 receptor beta-arrestin 2 interaction: a high-affinity receptor phenotype. *Mol. Endocrinol.* **19**, 812–823.
31 Sonoda N, Imamura T, Yoshizaki T, Babendure JL, Lu J-C & Olefsky JM (2008) Beta-Arrestin-1 mediates glucagon-like peptide-1 signaling to insulin secretion in cultured pancreatic beta cells. *Proc Natl Acad Sci USA* **105**, 6614–6619.
32 Buenaventura T, Bitsi S, Laughlin WE, Burgoyne T, Lyu Z, Oqua AI, Norman H, McGlone ER, Klymchenko AS, Corrêa IR, Walker A, Inoue A, Hanyaloglu A, Grimes J, Koszegi Z, Calebiro D, Rutter GA, Bloom SR, Jones B & Tomas A (2019) Agonist-induced membrane nanodomain clustering drives GLP-1 receptor responses in pancreatic beta cells. *PLoS Biol* **17**, e3000097.
33 Zhu L, Rossi M, Cui Y, Lee RJ, Sakamoto W, Perry NA, Urs NM, Caron MG, Gurevich VV, Godlewski G, Kunos G, Chen M, Chen W & Wess J (2017) Hepatic β-arrestin 2 is essential for maintaining euglycemia. *J Clin Invest* **127**, 2941–2945.
34 Abdullah N, Beg M, Soares D, Dittman JS & McGraw TE (2016) Downregulation of a GPCR by β-Arrestin2-Mediated Switch from an Endosomal to a TGN Recycling Pathway. *Cell Rep* **17**, 2966–2978.
35 Levoye A, Zwier JM, Jaracz-Ros A, Klipfel L, Cottet M, Maurel D, Bdioui S, Balabanian K, Prézeau L, Trinquet E, Durroux T & Bachelerie F (2015) A Broad G Protein-Coupled Receptor Internalization Assay that Combines SNAP-Tag Labeling, Diffusion-Enhanced Resonance Energy Transfer, and a Highly Emissive Terbium Cryptate. *Front Endocrinol (Lausanne)* **6**, 167.

36 Buenaventura T, Kanda N, Douzenis PC, Jones B, Bloom SR, Chabosseau P, Corrêa IR, Bosco D, Piemonti L, Marchetti P, Johnson PR, Shapiro AMJ, Rutter GA & Tomas A (2018) A Targeted RNAi Screen Identifies Endocytic Trafficking Factors That Control GLP-1 Receptor Signaling in Pancreatic β-Cells. *Diabetes* **67**, 385–399.
37 Khajavi N, Finan B, Kluth O, Müller TD, Mergler S, Schulz A, Kleinau G, Scheerer P, Schürmann A, Gudermann T, Tschöp MH, Krude H, Dimarchi RD & Biebermann H (2018) An incretin-based tri-agonist promotes superior insulin secretion from murine pancreatic islets via PLC activation. *Cell. Signal.* **51**, 13–22.
38 Svendsen B, Larsen O, Gabe MBN, Christiansen CB, Rosenkilde MM, Drucker DJ & Holst JJ (2018) Insulin Secretion Depends on Intra-islet Glucagon Signaling. *Cell Rep* **25**, 1127–1134.e2.
39 Clemmensen C, Finan B, Müller TD, Dimarchi RD, Tschöp MH & Hofmann SM (2019) Emerging hormonal-based combination pharmacotherapies for the treatment of metabolic diseases. *Nat Rev Endocrinol* **15**, 90–104.
40 Runge S, Schimmer S, Oschmann J, Schiødt CB, Knudsen SM, Jeppesen CB, Madsen K, Lau J, Thøgersen H & Rudolph R (2007) Differential structural properties of GLP-1 and exendin-4 determine their relative affinity for the GLP-1 receptor N-terminal extracellular domain. *Biochemistry* **46**, 5830–5840.
41 Montrose-Rafizadeh C, Yang H, Rodgers BD, Beday A, Pritchette LA & Eng J (1997) High potency antagonists of the pancreatic glucagon-like peptide-1 receptor. *Journal of Biological Chemistry* **272**, 21201–21206.
42 Graaf C de, Donnelly D, Wootten D, Lau J, Sexton PM, Miller LJ, Ahn J-M, Liao J, Fletcher MM, Yang D, Brown AJH, Zhou C, Deng J & Wang M-W (2016) Glucagon-Like Peptide-1 and Its Class B G Protein-Coupled Receptors: A Long March to Therapeutic Successes. *Pharmacol Rev* **68**, 954–1013.
43 Unson CG, Andreu D, Gurzenda EM & Merrifield RB (1987) Synthetic peptide antagonists of glucagon. *Proc Natl Acad Sci USA* **84**, 4083–4087.
44 Hansen LS, Sparre-Ulrich AH, Christensen M, Knop FK, Hartmann B, Holst JJ & Rosenkilde MM (2016) N-terminally and C-terminally truncated forms of glucose-dependent insulinotropic polypeptide are high-affinity competitive antagonists of the human GIP receptor. *Br J Pharmacol* **173**, 826–838.
45 Mentlein R, Gallwitz B & Schmidt WE (1993) Dipeptidyl-peptidase IV hydrolyses gastric inhibitory polypeptide, glucagon-like peptide-1(7-36)amide, peptide histidine methionine and is responsible for their degradation in human serum. *Eur. J. Biochem.* **214**, 829–835.
46 Hareter A, Hoffmann E, Bode HP, Göke B & Göke R (1997) The positive charge of the imidazole side chain of histidine7 is crucial for GLP-1 action. **44**, 701–705.
47 Deacon CF, Knudsen LB, Madsen K, Wiberg FC, Jacobsen O & Holst JJ (1998) Dipeptidyl peptidase IV resistant analogues of glucagon-like peptide-1 which have extended metabolic stability and improved biological activity. *Diabetologia* **41**, 271–278.
48 Sarrauste de Menthière C, Chavanieu A, Grassy G, Dalle S, Salazar G, Kervran A, Pfeiffer B, Renard P, Delagrange P, Manechez D, Bakes D, Ktorza A & Calas B (2004) Structural requirements of the N-terminal region of GLP-1-[7-37]-NH2 for receptor interaction and cAMP production. *Eur J Med Chem* **39**, 473–480.
49 Hinke SA, Gelling R, Manhart S, Lynn F, Pederson RA, Kühn-Wache K, Rosche F, Demuth H-U, Coy D & McIntosh CHS (2003) Structure-activity relationships of glucose-dependent insulinotropic polypeptide (GIP). *Biol. Chem.* **384**, 403–407.
50 Gault VA, Flatt PR, Harriott P, Mooney MH, Bailey CJ & O'Harte FPM (2003) Improved biological activity of Gly2- and Ser2-substituted analogues of glucose-dependent insulinotrophic polypeptide. *J Endocrinol* **176**, 133–141.
51 Ismail S, Gherardi M-J, Froese A, Zanoun M, Gigoux V, Clerc P, Gaits-Iacovoni F, Steyaert J, Nikolaev VO & Fourmy D (2016) Internalized Receptor for Glucose-dependent Insulinotropic Peptide stimulates adenylyl cyclase on early endosomes. *Biochem. Pharmacol.* **120**, 33–45.
52 Hupe-Sodmann K, McGregor GP, Bridenbaugh R, Göke R, Göke B, Thole H, Zimmermann B & Voigt K (1995) Characterisation of the processing by human neutral endopeptidase 24.11 of

GLP-1(7-36) amide and comparison of the substrate specificity of the enzyme for other glucagon-like peptides. *Regul Pept* **58**, 149–156.
53 Lu J & Willars GB (2019) Endothelin-converting enzyme-1 regulates glucagon-like peptide-1 receptor signalling and resensitisation. *Biochem J* **476**, 513–533.
54 Bugliani M, Syed F, Paula FMM, Omar BA, Suleiman M, Mossuto S, Grano F, Cardarelli F, Boggi U, Vistoli F, Filipponi F, De Simone P, Marselli L, De Tata V, Ahrén B, Eizirik DL & Marchetti P (2018) DPP-4 is expressed in human pancreatic beta cells and its direct inhibition improves beta cell function and survival in type 2 diabetes. *Mol Cell Endocrinol* **473**, 186–193.
55 Malm-Erjefält M, Bjørnsdottir I, Vanggaard J, Helleberg H, Larsen U, Oosterhuis B, van Lier JJ, Zdravkovic M & Olsen AK (2010) Metabolism and excretion of the once-daily human glucagon-like peptide-1 analog liraglutide in healthy male subjects and its in vitro degradation by dipeptidyl peptidase IV and neutral endopeptidase. *Drug Metab. Dispos.* **38**, 1944–1953.

Figure legends

Figure 1. Biased incretin analogues with N-terminal region substitutions. (**A**) cAMP responses in PathHunter CHO-GLP-1R, CHO-GIPR or CHO-GCGR cells (as appropriate) to analogues of GLP-1, GIP and GCG, 30-minute stimulation, *n*=5, 4-parameter fits of pooled data shown. (**B**) As for (A) but β-arrestin-2 recruitment responses. (**C**) The relative impact of each amino acid substitution on cAMP signalling is shown by subtracting Log τ/K_A for the reference agonist (GLP-1, GIP or GCG) from that of each analogue on a per-assay basis. (**D**) As for (C) but for β-arrestin-2 recruitment. (**E**) Signal bias for N-terminally modified GLP-1, GIP and GCG analogues at their cognate receptors, calculated as normalised log transduction ratios [$\Delta\Delta\log(\tau/K_A)$] relative to GLP-1, GIP or GCG, respectively. The numerical degree of bias is indicated for each ligand after anti-log transform. Data are represented as mean ± SEM, except for bias plots, where error bars indicate 95% confidence intervals. Parameter estimates for concentration responses are provided in Table 2.

Figure 2. Internalisation properties of GLP-1, GIP, GCG, and their derivatives. (**A**) Internalisation of SNAP-GLP-1R, SNAP-GIPR and SNAP-GCGR stimulated, respectively, by 100 nM agonist (or vehicle) in HEK293T cells, measured by DERET, *n*=4. (**B**) Time course showing internalisation of SNAP-GLP-1R, SNAP-GIPR or SNAP-GCGR in response to, respectively, 100 nM GLP-1, GIP or GCG, measured by reversible SNAP-tag labelling in transiently transfected HEK293T cells, *n*=5. (**C**) Representative images of transiently transfected HEK293T cells labelled with BG-S-S-649 (1 μM) and treated ± 100 nM GLP-1, GIP or GCG, imaged before and after removal of residual surface BG-S-S-649 using Mesna; scale bar = 16 μm. The same brightness and contrast settings are applied for all images. (**D**) SNAP-GLP-1R internalisation in CHO-K1 cells treated with indicated agonist (100 nM), measured by DERET, *n*=4, AUC *versus* GLP-1 compared by randomised block ANOVA with Dunnett's test. (**E**) SNAP-GIPR internalisation in CHO-K1 cells treated with indicated agonist (100 nM), measured by DERET, *n*=4, AUC *versus* GIP compared by one-way randomised block ANOVA with Dunnett's test. (**F**) Representative images showing GLP-1R and GIPR agonist-mediated internalisation of their cognate receptor, with quantification below from *n*=5 experiments and

comparison by one-way randomised block ANOVA with Dunnett's test; scale bar = 26 μm. * $p<0.05$ by statistical test indicated in the text. Data represented as mean ± SEM, or as individual replicates.

Figure 3. Responses in INS-1 832/3 cells. (**A**) Expression of *Glp1r*, *Gipr* and *Gcgr* in INS-1 832/3 cells, determined by qPCR, normalised to expression of endogenous control gene 18S by $2^{-\Delta Ct}$, *n*=2. (**B**) Insulin secretory responses in INS-1 832/3 cells treated for 16 hours with GLP-1 analogues at 11 mM glucose, *n*=5, 3-parameter fits shown. (**C**) As for (B) but with GIP analogues. (**D**) Correlation of GLP-1 and GIP analogue maximum insulin secretion and maximum β-arrestin-2 recruitment (Figure 1) by linear regression. (**E**) Insulin secretory responses in wild-type and GLP-1R KO INS-1 832/3 cells treated for 16 hours with GCG analogues at 11 mM glucose, *n*=5, 3-parameter fits shown. Data represented as mean ± SEM. Parameter estimates for concentration responses are provided in Table 3.

Figure 4. Responses in Huh7 cells and primary hepatocytes. (**A**) cAMP responses to GCG analogues in Huh7-GCGR cells treated for 16 hours, relative to response to forskolin (10 min, 10 μM), *n*=4, 4-parameter fits shown. (**B**) Effect of prolonged (16-hour) exposure to indicated agonist (10 nM) on upregulation of *G6pc* in Huh7-GCGR cells, *n*=4. (**C**) Effect of prolonged (16-hour) exposure to indicated agonist (100 nM) on glucose production by primary mouse hepatocytes, *n*=4, expressed as fold change to vehicle stimulation. For (B) and (C), no treatment response was significantly different to that of GCG, by one-way randomised block ANOVA with Dunnett's test. Error bars indicate SEM. Parameter estimates for concentration responses are provided in Table 3.

Figure 1

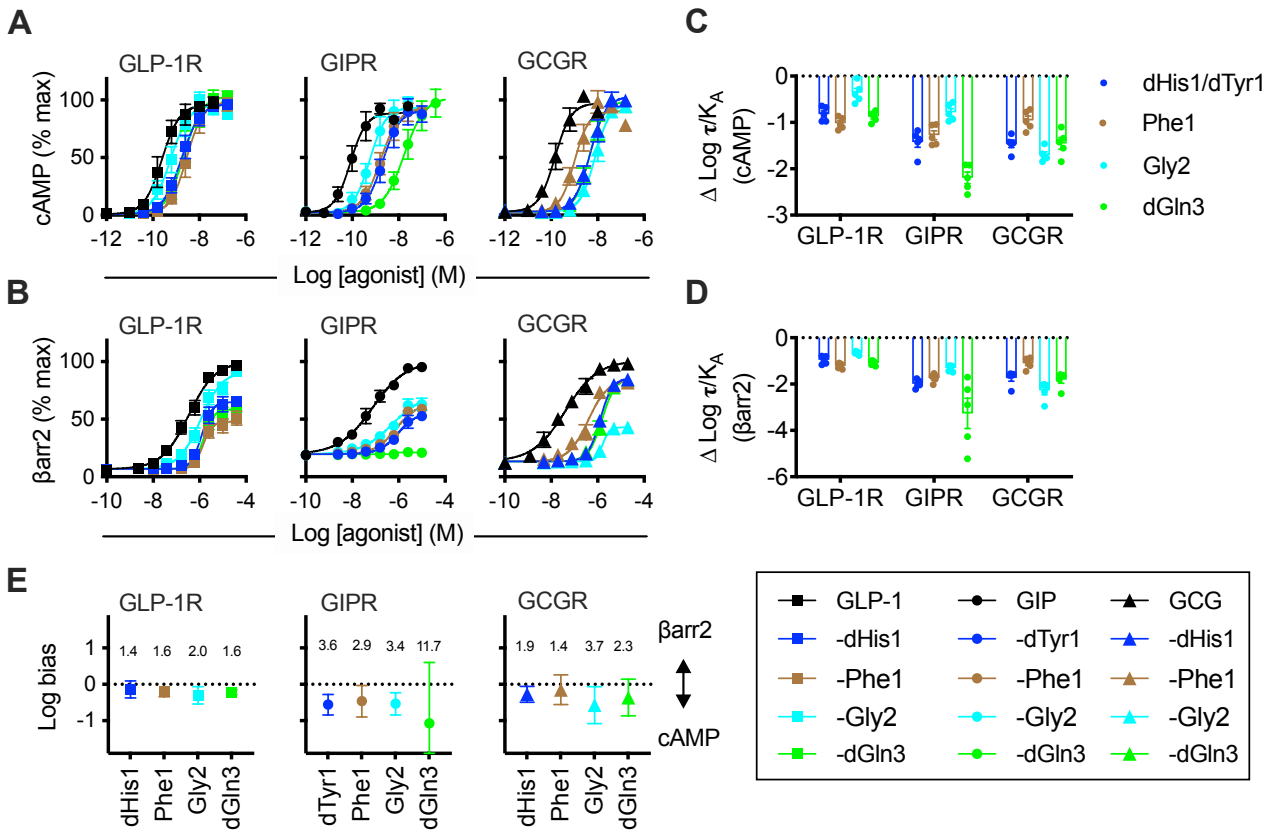
A
GLP-1R
GIPR
GCGR
cAMP (% max)
100
50
0
-12 -10 -8 -6
Log [agonist] (M)
B
βarr2 (% max)
-10 -8 -6 -4
C
Δ Log τ/K_A (cAMP)
0
-1
-2
-3
GLP-1R GIPR GCGR
dHis1/dTyr1
Phe1
Gly2
dGln3
D
Δ Log τ/K_A (βarr2)
-4
-6
E
Log bias
1.4 1.6 2.0 1.6
3.6 2.9 3.4 11.7
1.9 1.4 3.7 2.3
dHis1 Phe1 Gly2 dGln3
dTyr1 Phe1 Gly2 dGln3
βarr2
cAMP
GLP-1
-dHis1
-Phe1
-Gly2
-dGln3
GIP
-dTyr1
-Phe1
-Gly2
-dGln3
GCG
-dHis1
-Phe1
-Gly2
-dGln3

Figure 2

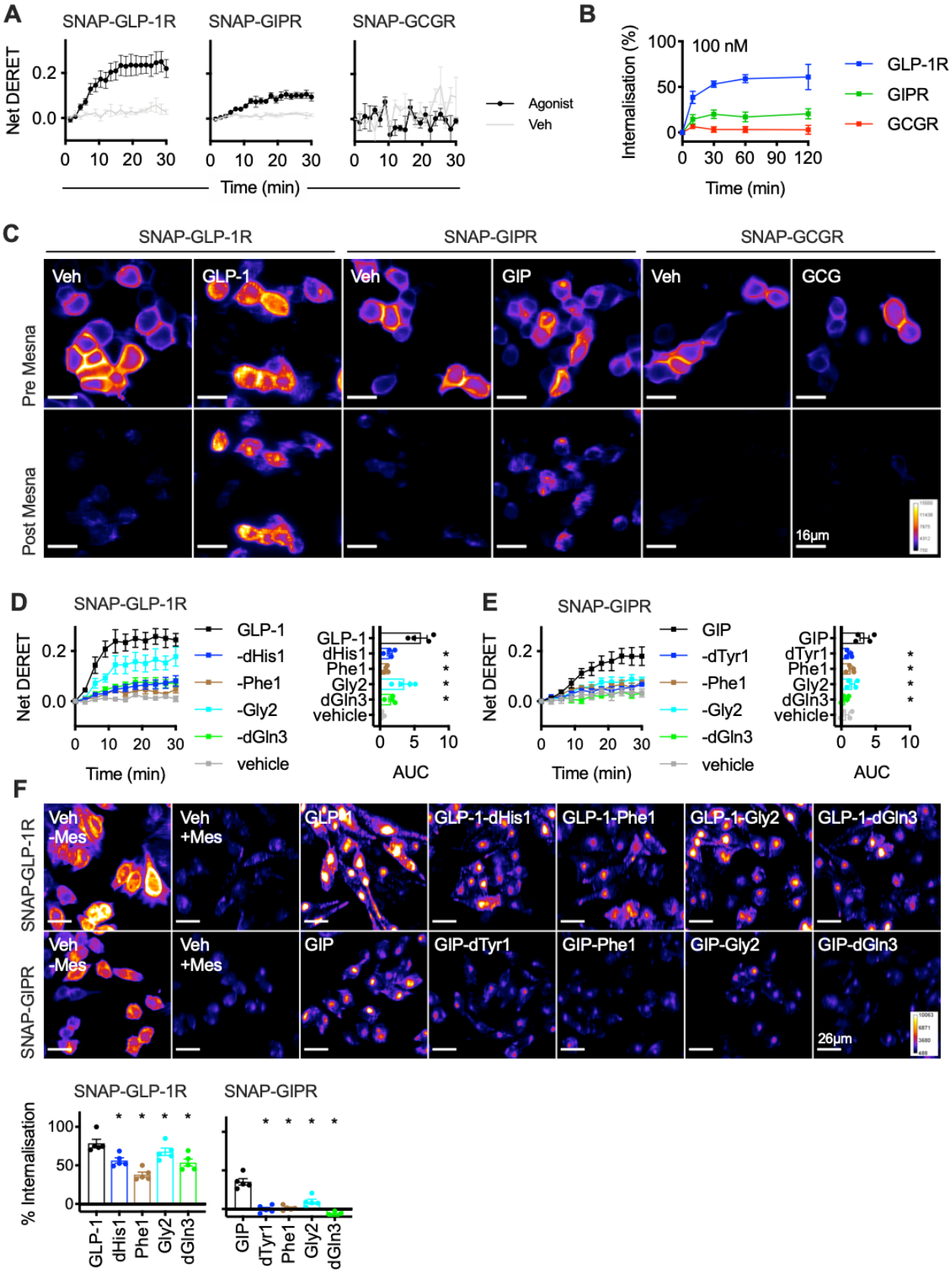
A
SNAP-GLP-1R
SNAP-GIPR
SNAP-GCGR
Net DERET
0.2
0.0
0 10 20 30
Time (min)
Agonist
Veh
B
Internalisation (%)
100
50
0
100 nM
0 30 60 90 120
Time (min)
GLP-1R
GIPR
GCGR
C
SNAP-GLP-1R
SNAP-GIPR
SNAP-GCGR
Pre Mesna
Post Mesna
Veh
GLP-1
GIP
GCG
16µm
D
SNAP-GLP-1R
Net DERET
Time (min)
GLP-1
-dHis1
-Phe1
-Gly2
-dGln3
vehicle
AUC
E
SNAP-GIPR
GIP
-dTyr1
F
SNAP-GLP-1R
SNAP-GIPR
Veh -Mes
Veh +Mes
GLP-1
GLP-1-dHis1
GLP-1-Phe1
GLP-1-Gly2
GLP-1-dGln3
GIP
GIP-dTyr1
GIP-Phe1
GIP-Gly2
GIP-dGln3
26µm
% Internalisation
100
50
0
GLP-1
dHis1
Phe1
Gly2
dGln3
GIP
dTyr1

Figure 3

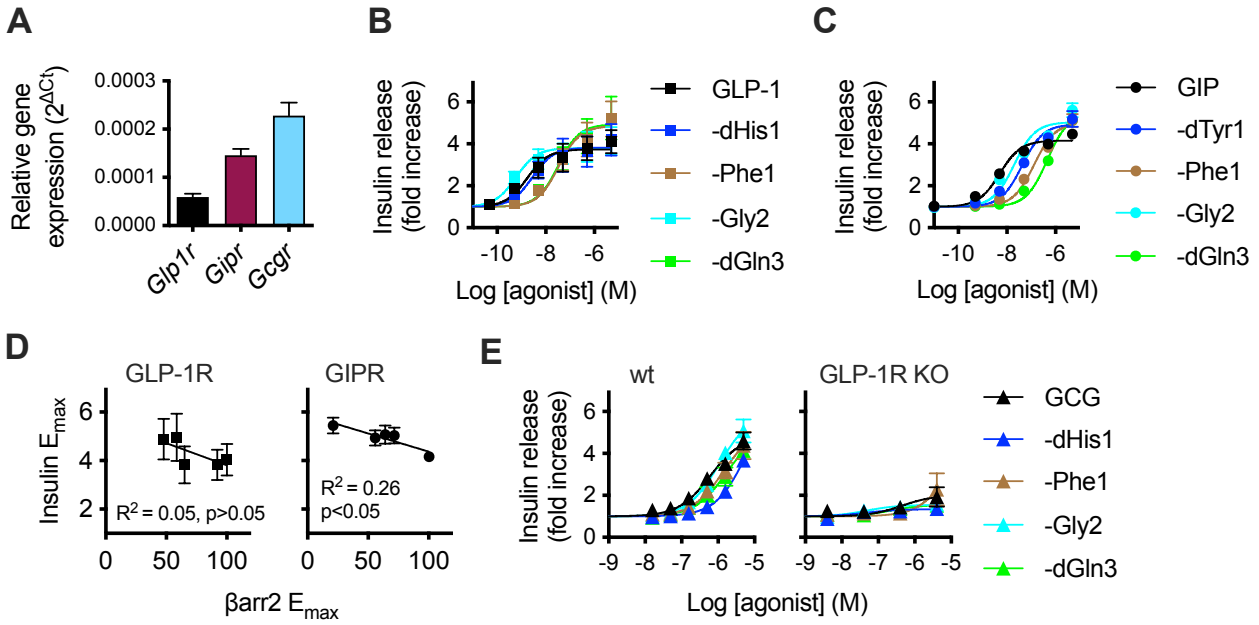
A
Relative gene expression ($2^{\Delta Ct}$)
0.0003
0.0002
0.0001
0.0000
Glp1r
Gipr
Gcgr
B
Insulin release (fold increase)
Log [agonist] (M)
GLP-1
-dHis1
-Phe1
-Gly2
-dGln3
C
Insulin release (fold increase)
Log [agonist] (M)
GIP
-dTyr1
-Phe1
-Gly2
-dGln3
D
GLP-1R
GIPR
Insulin E_{max}
R^2 = 0.05, p>0.05
R^2 = 0.26
p<0.05
βarr2 E_{max}
E
wt
GLP-1R KO
Insulin release (fold increase)
Log [agonist] (M)
GCG
-dHis1
-Phe1
-Gly2
-dGln3

Figure 4

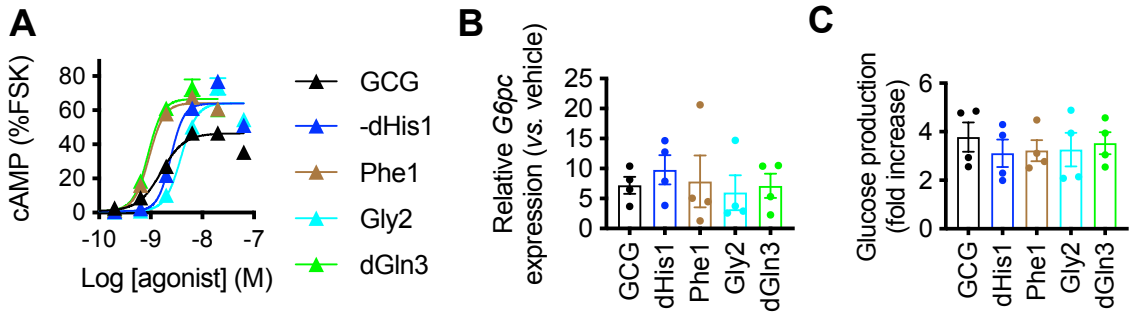
A
cAMP (%FSK)
80
60
40
20
0
-10
-9
-8
-7
Log [agonist] (M)
GCG
-dHis1
Phe1
Gly2
dGln3
B
Relative G6pc expression (vs. vehicle)
25
20
15
10
5
0
GCG
dHis1
Phe1
Gly2
dGln3
C
Glucose production (fold increase)
6
4
2
0
GCG
dHis1
Phe1
Gly2
dGln3